



Numerical simulation and measurements of acoustic transmissions from Heard Island to the equatorial Indian Ocean

S Prasanna Kumar, G S Navelkar, T V Ramana Murty, Y K Somayajulu, A K Saran & C S Murty
National Institute of Oceanography, Dona Paula, Goa-403 004, India
Received 20 March 1995; revised 29 January 1996

Simulated acoustic propagation showed a gradual deepening of the ray paths from the southern ocean towards tropics. Also the axis of the sound channel deepens from 150 m to 1600 m. Sudden jumps were noticed in the acoustic ray paths in the vicinity of the Sub Tropical Convergence. Measured acoustic signals, received at the Indian listening station has a signal to noise ratio (SNR) of 20 dB on an average and confirmed their detectability over distances as far as 7000 km. The phase stability of these signals allowed coherent averaging time of 20 minutes for corresponding increase in the SNR. Measured intensity losses were about 135 dB in contrast to those computed values of 150 dB.

Heard Island experiment, was conducted during early 1991, to test the novel idea of acoustically measuring the global ocean warming put forward by Munk & Forbes¹. The measurements of strength and stability of acoustic signals at different listening stations in this experiment were proposed to examine the feasibility of installing permanent sources and receivers round the world ocean for long-term monitoring.

The present paper deals with the results of the analysis of acoustic propagation paths from the source near the Heard Island site to the Indian receiving station based on the numerical simulation and processing of received signals. Signal strength and phase stability of the receptions have also been discussed.

Materials and Methods

Sound speed computations

The climatological hydrographic data in the Indian Ocean between longitudes 69.5°-74.5° E and latitudes 55.5° S-13.5° N, at 1 degree intervals have been derived from the Levitus² atlas. Temperature and salinity values at all standard depths were used in the computation of sound speeds using the empirical relation of Chen & Millero³. The simplified form of this is as given below.

$$c(s,t,p) = c_w(t,p) + A(t,p)s + B(t,p)s^{3/2} + D(t,p)s^2$$

where p = pressure (in decibars),
 t = temperature (degree celcius),
 s = salinity (pss),
 c = sound speed (meters/sec.)

For determining the depth of the sound channel axis (minimum sound speed layer), the vertical sound speeds at 10 m depth intervals were obtained through weighted parabolic interpolation which enabled pick up this layer precisely. Mean sound speed profiles (for longitudes 69.5°-74.5° E) at 1° intervals in the meridional direction along the track were obtained. In all, about 66 profiles were used to study the spatial sound speed structure in the meridional direction and also used as basic input to run the ray model.

Numerical simulations were carried out, to determine the receiver location and signal strength for keeping the Indian listening station, based on the climatological data. Sound speed profiles were interpolated at every 25 km range, for the model simulation of propagation. It is used as input for a range-dependent ray trace program⁴ to trace acoustic rays over a propagation range of about 7000 km.

Experimental set-up

The acoustic source, used for the experiment, was kept at a site 40 nautical miles southeast of the Heard Island (53° 15' S, 73° 40' E) in the Indian Ocean sector of Antarctica⁴ (Fig. 1, inset). The source consisted of a vertical array of transducers lowered from *R/V Cory Chouest* to a depth of 150 m below the surface, coinciding with the axis of the sound channel. Different types of continuous wave (CW) and phase coded signals centered at a frequency of 57 Hz were transmitted for one hour transmission at every three hours round the clock (Table 1) from 0000 GMT on 26 January through 2100 GMT on 31 January. Due to mechanical problems transmissions were stopped in between from 1600 GMT on 27 January to 0800 GMT

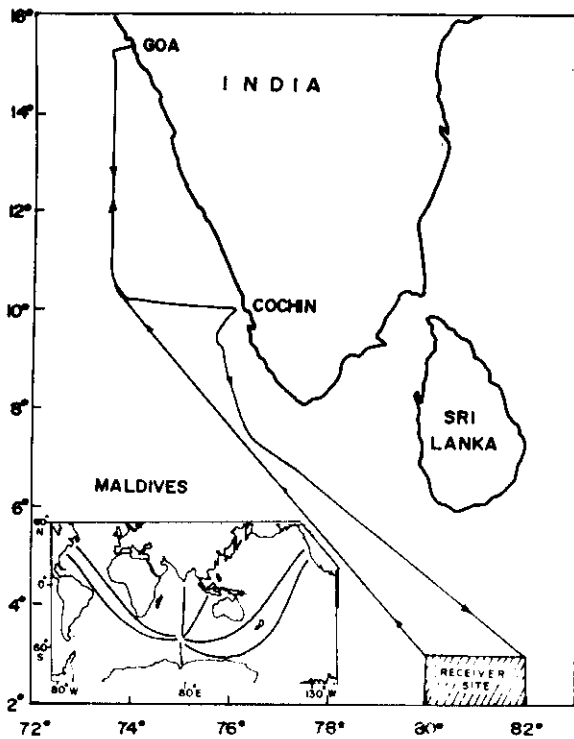


Fig. 1—Location of Indian receiving station and refracted geodesic path from Heard Island to receiver locations.

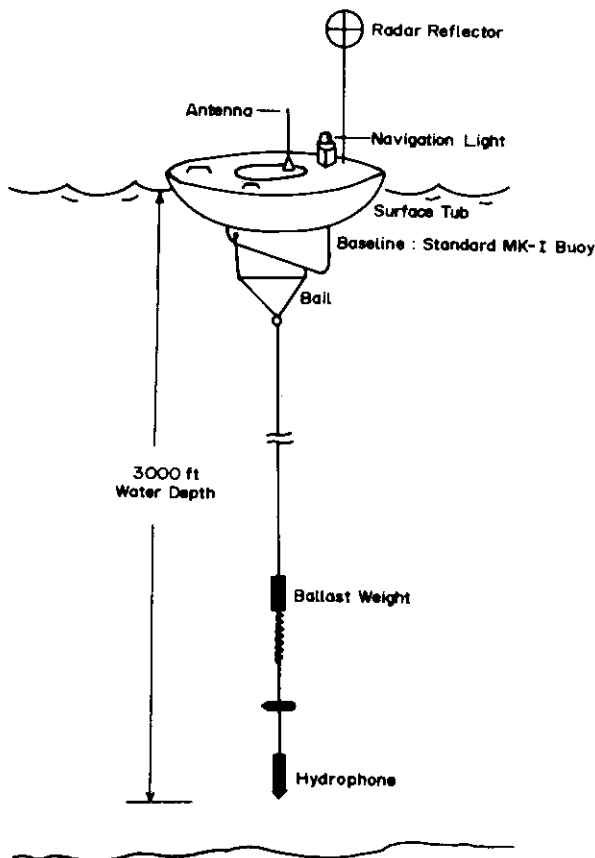


Fig. 2—Schematic diagram of the drifting buoy.

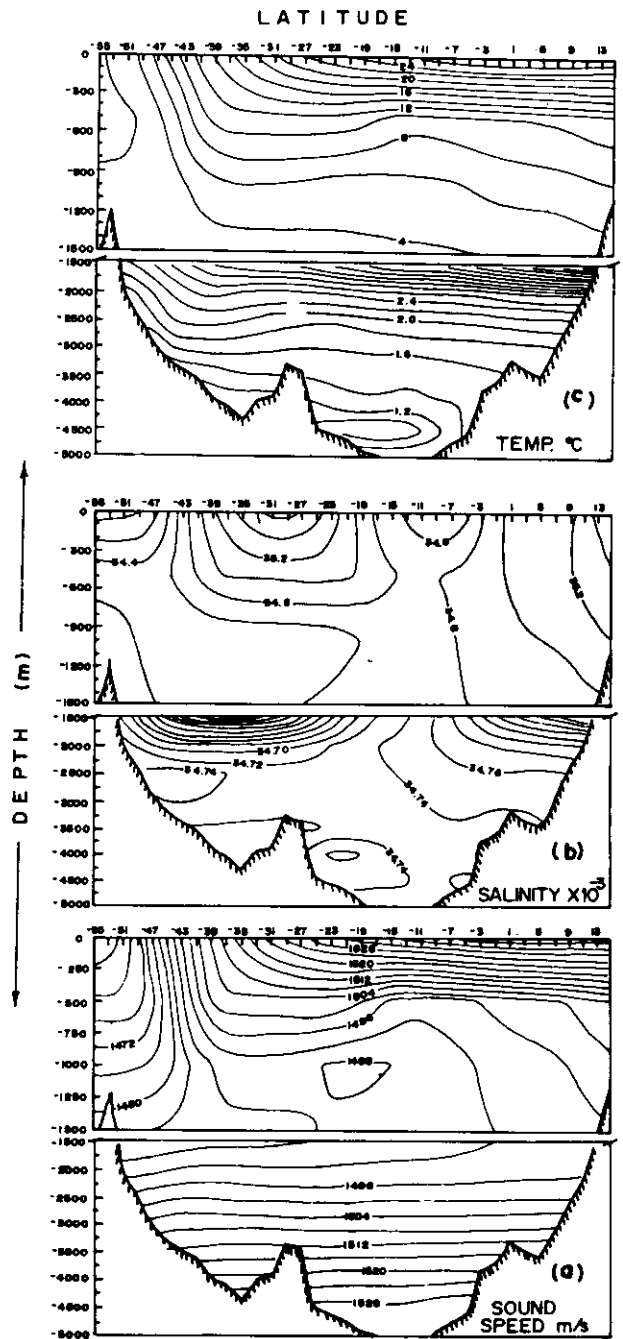


Fig. 3—Vertical sections along 71° E.

on 28 January and 2200 GMT on 28 January to 2300 GMT on 29 January, 1991.

The Indian Ocean receiving station (Fig. 1) consisted of a recoverable Spartan 51-A buoy (Fig. 2) and expendable Magnavox 41-B sonobuoy(s) for receiving the signals, the latter served as backups to the former. A radio receiver onboard *ORV Sagar Kanya* monitored and received data from the buoy using a PC. The received data could be monitored in real time for signal reception while the data was being

Table 1—Signal transmission and reception details

Tr. time (GMT)	Signal type	Rt. time (GMT)	Comments
26-01-1991			
0000	CW	0124	signal received with SNR around 26 dB
0300	3/10 pentaline	0357	clear signal received with 3 peaks
0600	255/5 m sequence	0658	signal not received-hydrophone fault
0900	1023/5 m sequence		-do-
1200	CW		-do-
1500	3/10 pentaline	1627	signal received with peak at 56.94 Hz
1800	255/5 m sequence	1857	signal received with SNR around 10 dB
2100	2048/5 m sequence	2157	signal received with SNR around 20 dB
27-01-1991			
0000	CW		sonobuoys not deployed
0300	3/10 pentaline		-do-
0600	255/5 m sequence		-do-
0900	511/5 m sequence	1005	signal received with SNR around 8 dB
1200	CW	1303	signal received with SNR around 24 dB
1500	3/10 pentaline	1557	signal received with SNR around 12 dB
29-01-1991			
0900	1023/5 m sequence	0957	signal received
1200	CW	1257	signal received with SNR around 15 dB
1500	3/10 pentaline	1557	pentaline spectral peaks with SNR = 24 dB
1800	255/5 m sequence	1857	signal received with SNR around 9 dB
2100	2048/5 m sequence		sonobuoy not deployed.
30-01-1991			
0000	CW		sonobuoy failed
0300	3/10 pentaline	0357	signal received with SNR around 20 dB
0600	255/5 m sequence	0657	signal received with noise peak at 50 Hz
0900	511/5 m sequence	0957	ship RT interference with signal
1200	CW	1257	low signal due to less elements active(2)
1500	3/10 pentaline	1557	-do-
1800	255/5 m sequence	1857	signal received with noise peak at 50 Hz
2100	1023/5 m sequence		sonobuoy not deployed
31-01-1991			
0000	CW		ship on transit, sonobuoy not deployed
0300	3/10 pentaline		-do-
0600	255/5 m sequence		-do-
0900	2048/5 m sequence		-do-
1200	CW		-do-
1500	3/10 pentaline		-do-
1800	255/5 m sequence		-do-
2100	511/5 m sequence		-do-

received and stored on the hard disk in the background.

Results and Discussion

Sound speed structure, constructed based on the 66 profiles, along 71° E (Fig. 3a) shows significant changes in sound speed in the meridional direction. This may be due to the gradual increase of temperature from southern ocean towards the tropical region. Depth of the SOFAR channel axis also showed variation from 150 m near Heard Island

to 1600 m in the Arabian Sea. The overall surface sound speed varied by 80 m/s over 7000 km. The sudden change in the sound speed structure centered at 45°S (50-40° S) is associated with the Subtropical Convergence Zone, which is characterised by a rapid increase of temperature by about 8°C and salinity by 0.8 PSU (Fig. 3b, c) towards north.

The simulated ray geometry, for launch angles +8°, +5°, +2° and -10° (Fig. 4), depicts a gradual deepening of the ray path which is brought in by the increasing depth of the sound channel axis towards

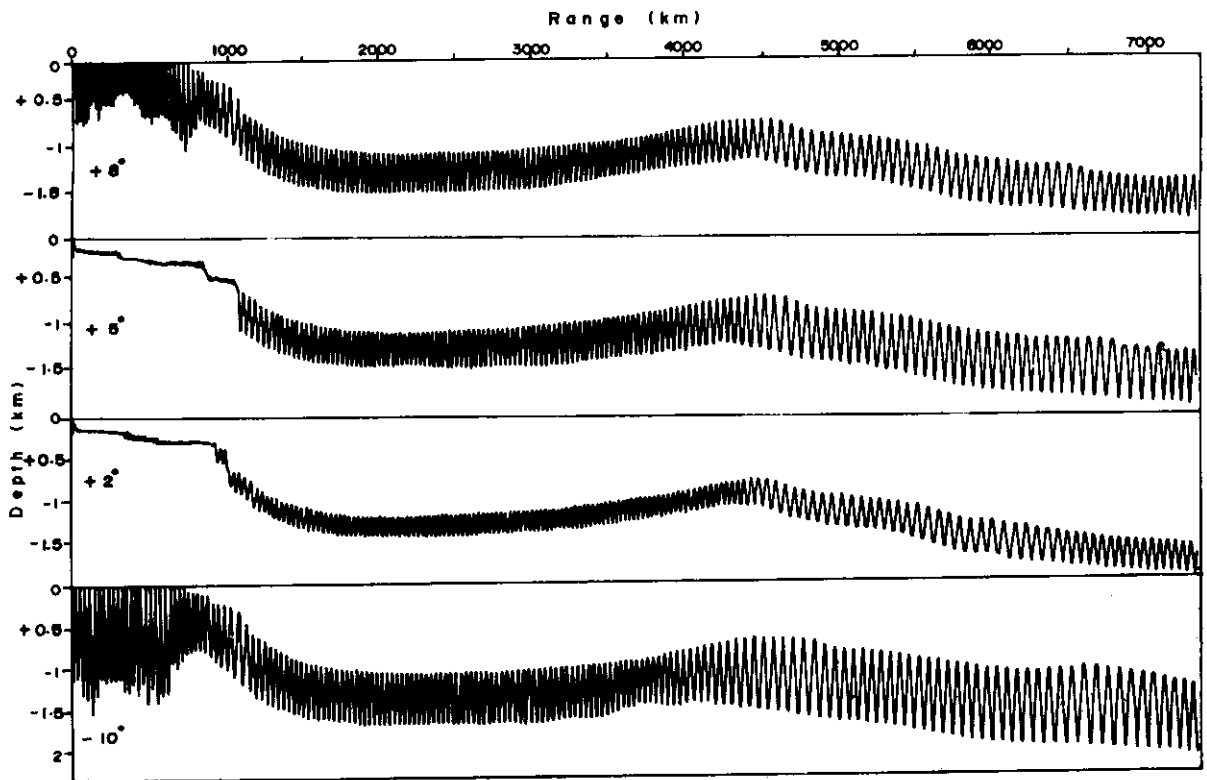


Fig. 4—Simulated acoustic ray paths for different launch angles from Heard Island to the Indian listening station.

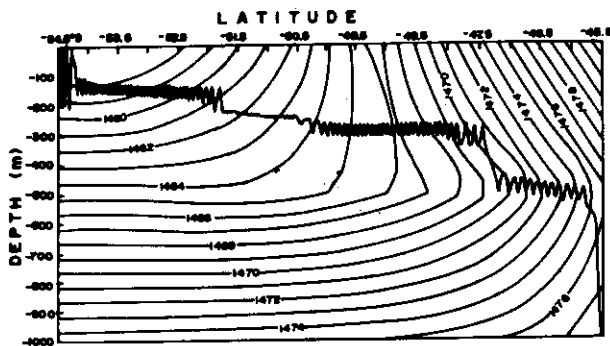


Fig. 5—Meridional sound speed structure across the Antarctic Convergence Zone along with acoustic ray path.

tropics. Close to the equator, the ray path shoals up by about 200 m, due to the strong divergence. Small angle rays confine close to the channel axis. Large angle rays undergo surface reflection due to the combined effect of low sound speeds at the top layer and shallow axis depth.

The sudden ray jumps prominently seen for rays with launch angles 5° and 2° at a range of 1000 km (Fig. 4) is associated with the rapid changes in the sound speed structure in the vicinity of Sub Tropical Convergence (Fig. 5). The ray travel times of these rays were of the order 1 hr. 18 min. The intensity losses due to spreading were calculated⁵ to be about 150 dB

while that estimated from the reception data was about 135 dB.

On line spectral analysis results are presented in Fig. 6. The peak at 50.46 Hz (Fig. 6c) is due to power line noise. Based on the FFT analysis some rough estimates were made about signal to noise ratio, and speculations as to the optimum coherent processing time. These conclusions are mainly drawn from cw and pentaline signals which contain distinct spectral peaks. During a CW reception (constant ambient noise), the deep sonobuoy signal is up to 20 dB stronger than the 41 B sonobuoy signal, for RMS spectra peaks. This might be attributed to the deeper sonobuoy's proximity to the sound channel axis and less noise in the bandpass range around 57 Hz at deeper depths. Two transmissions were received on the deep sonobuoy. The best signal to noise ratio received was nominally 40 dB on the deep sonobuoy when receiving CW. On the 41B Sonobuoy, a signal to noise ratio in the low to mid 20 dB range was obtained. The m sequence receptions had visible carrier spikes, but the peak signal to noise ratio was less as only half the energy is in the carrier. A doppler shift of -0.06 Hz to $+0.08$ Hz has been observed. Source ship and/or receiver drift could be a plausible cause for the observed doppler shift. Incidentally, the receiver ship drift trajectory (Fig. 7) monitored using the GPS

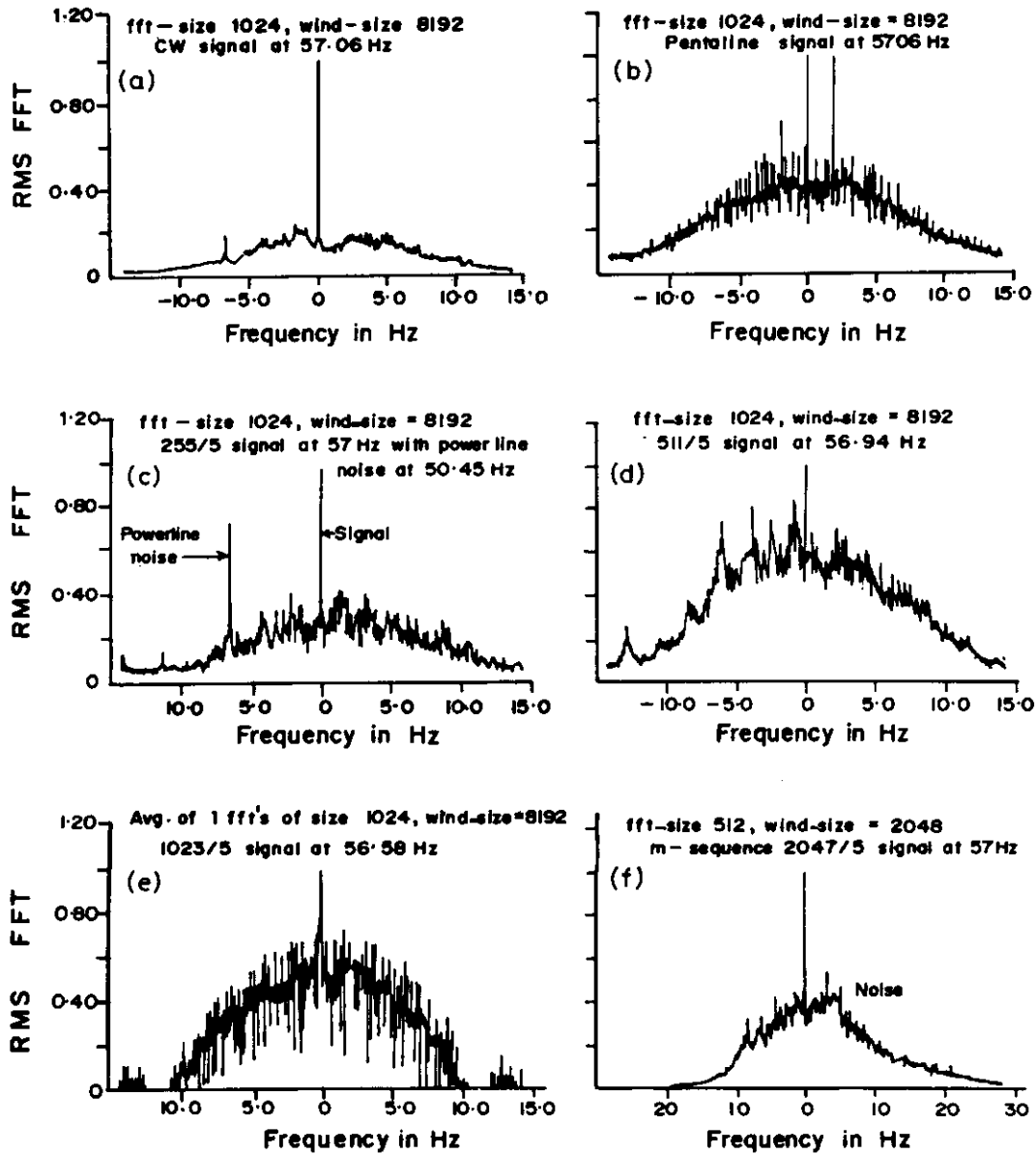


Fig. 6—FFT spectrum of the received signal indicating peaks for different types of transmissions

showed a prominent direction of drift towards southwest at the rate of 1.5 km/hr.

The received signals showed unexpected combination of phase stability and amplitude variability. When there were no transmissions the band pass filtered ambient noise of the ocean was recorded. This noise was found to be stable over the period of observation.

Off line processing of the entire data from the 11 receiving stations was done to determine the power, stability, time resolution and dispersions⁶. The Indian Ocean station data has been subjected to "Frequency domain analysis" of each transmission. A hamming window was used to reduce the frequency sidelobes

with 7/8 of the data common between the adjacent windows to enhance the continuity and follow quick changes.

The post processed data for a typical reception (CW signal at 1200 GMT on 27 January 1991, (Table 1) is presented in Fig. 8. All significant FFT magnitudes, which are more than 2.5 times the median of the magnitudes of the 47 Hz to 67 Hz band, are represented by dots of same size and darkness in the plot (Fig. 8a). Thus it represents the frequency spectrogram of the signal over the reception period. The other plots represents the bin shift, magnitude and residual phase of the carrier (Fig. 8b-d). The time (minutes) versus frequency (Hz) plot (Fig. 8a) shows

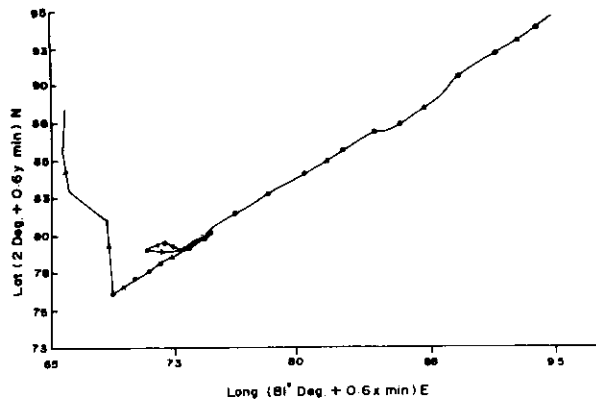


Fig. 7—Typical drift trajectory derived from GPS on board ORV Sagar Kanya.

Heard Island - Goa, File : g0271303.sam Ch. 1 Julian : 027 : 13 : 04 : 21

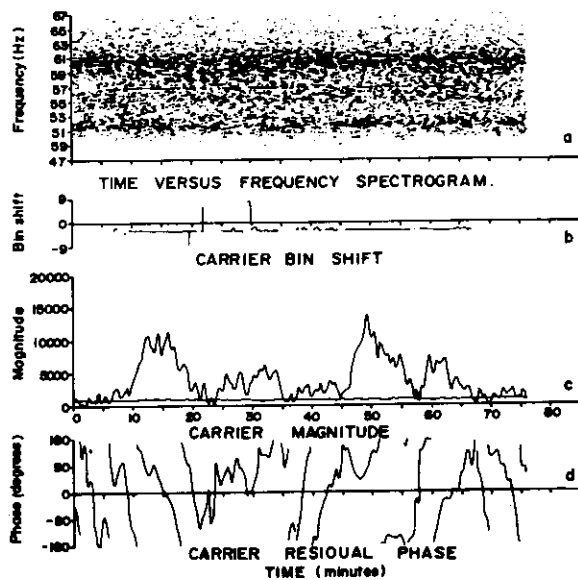


Fig. 8—Post processed data from the Indian receiving station.

prominent signal at about 57 Hz indicated by the continuous dots. The dark region in the spectrogram, spread around 60 Hz is due to the noise of the ship's generators. The bin shift (Fig. 8b) indicates the

presence of the doppler shifted carrier. The patches with straight line are the regions with stable carrier with constant doppler shift of about -0.1 Hz. The magnitudes of the carrier bin along with the median (Fig. 8c) shows the reception of the carrier. The fluctuations in the carrier magnitude was in part due to the multipath propagation and the variations in the number of active sources in the source array during the transmission period. The change in the phase of the carrier (Fig. 8d) elucidates the regions of constant doppler shift with linear phase change with time. In short, it is discernible from the above that the carrier with its doppler could be traced and monitored which is required for further processing like demodulation and cross-correlation.

Acknowledgement

The authors are grateful to the Director, NIO and the Department of Ocean Development, Govt. of India, New Delhi for their keen interest in this international collaborative program.

References

- 1 Munk WH & Forbes A M G, *J Phys Oceanogr.* 19 (1989) 1765.
- 2 Levitus S, *Climatological atlas of the world oceans*, NOAA professional paper, No 13, (U S Govt Printing Office, Washington D C) 1982, pp 173.
- 3 Chen C - T & Millero F J, *J Acoust Soc Am*, 60 (1977) 129.
- 4 Mahadevan R, Somayajulu Y K, Ramana Murty T V, Murty CS & Sastry J S, *Tomographic forward problem : Computational details for preparation of data kernel*. TR-NIO 7-89 (National Institute of Oceanography, Goa) 1989, pp 30.
- 5 Ramana Murty T V, Somayajulu Y K & Sastry J S, *Indian J Mar Sci.* 19 (1990) 235.
- 6 Metzger K, Dzieciuch M & Birdsall T G, *Heard Island feasibility test data survey in the frequency domain*. (University of Michigan, USA) 1991.
- 7 Munk WH, Spindel R C, Baggeroer A & Birdsall T G, *J Acoust Soc Am*, 96 (1994) 2330.